Electronic Supplementary Material (ESI) for Molecular Systems Design & Engineering.

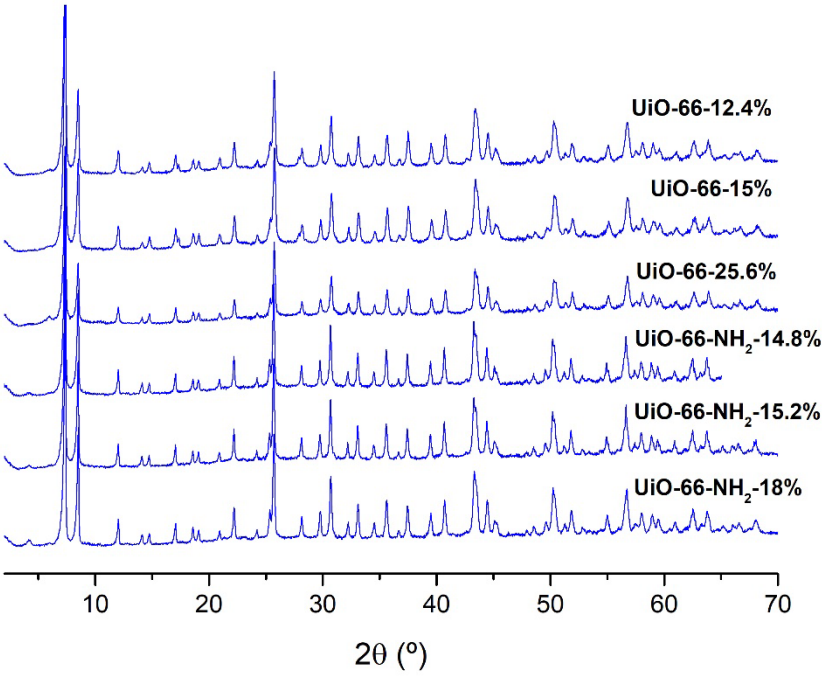

Figure S1. XRD patterns of UiO-66-X and UiO-66-NH_2-X with different amount of linker defects X (%)

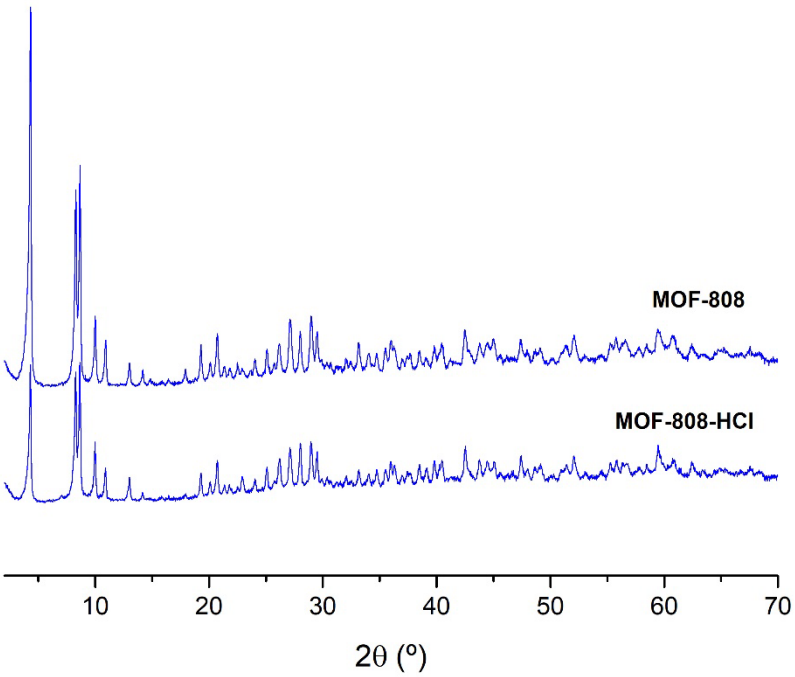

Figure S2. XRD patterns of MOF-808 and MOF-808-HCl

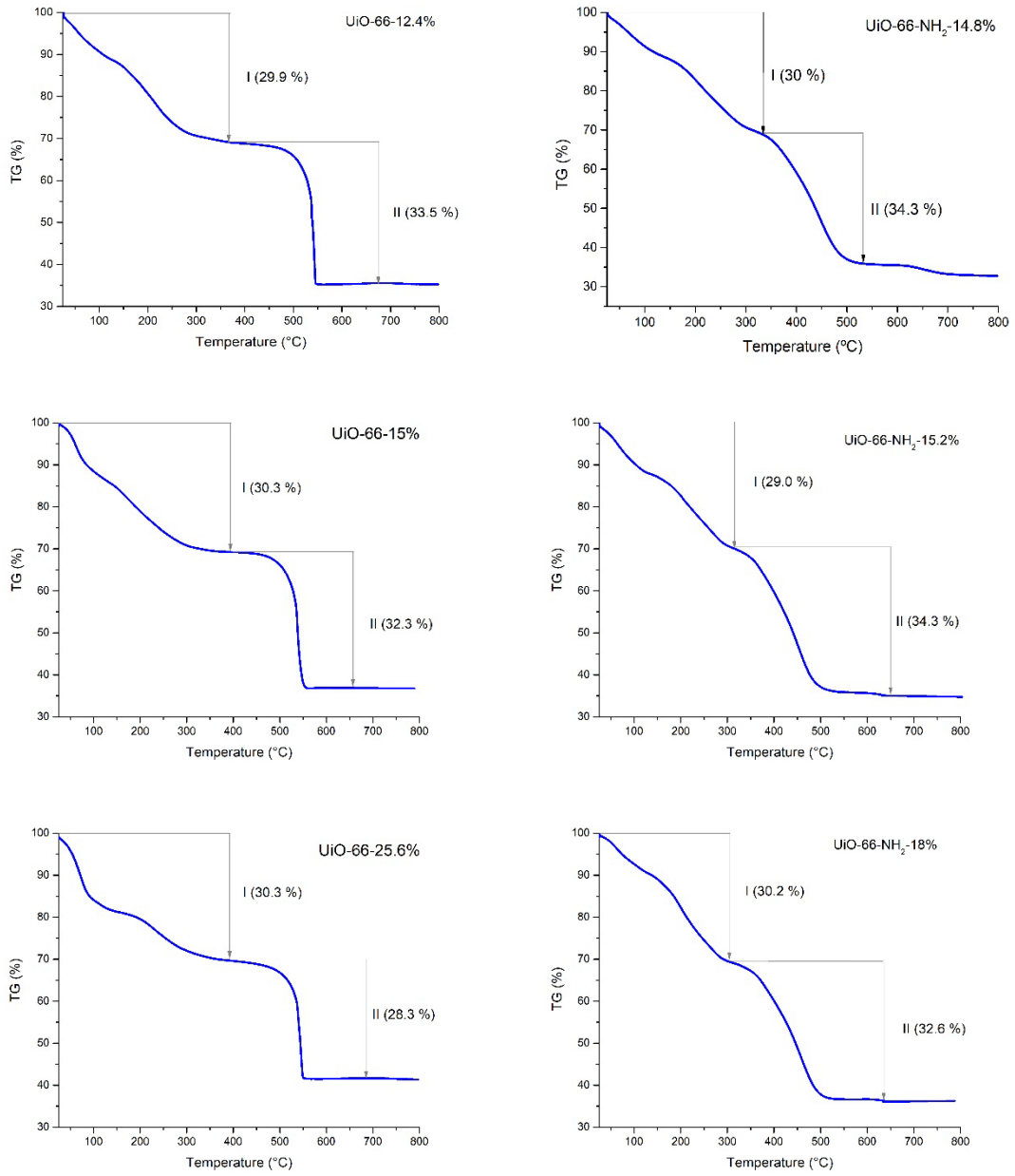

Figure S3. Thermograms of UiO-66-X and UiO-66-NH_2-X samples with different amount of linker defects: ***I***-water and solvent weight loss; ***II*** – organic ligand weight loss

Determination of the amount of missing linkers in UiO-66

The percentage of linker defects was calculated following the method proposed by Valenzano[1] using TG data (Figure S3). When UiO-66 is dehydrated and dehydroxylated (in the range of 300-500 °C according to TGA) its structure corresponds to the formula $ZrO(CO_2)_2(C_6H_4)$. Assuming that only ZrO_2 is formed as residue at high temperature (500-550 °C), it is possible to calculate

the experimental weight loss corresponding to the organic linker using TG analysis and compare it with the theoretical weight loss expected from the ideal structure of UiO-66.

In this way, the percentage of linker defects and the coordination number of the Zr_6 clusters (CN) can be calculated using the following equations:

$$\%\, defect\ sites = \left(1 - \frac{wt.\%\ real}{wt.\%\ theor}\right) x\ 100$$

$$CN = 12\ x \left(1 - \frac{\%defect\ sites}{100}\right)$$

where *% defect sites* corresponds to the amount of missing linkers (BDC) of UiO-66; *wt.% exp.* is the weight loss of UiO-66 associated to BDC linkers determined from TG experimental data; *wt.% theor* corresponds to the amount of BDC linkers calculated for stoichiometrically perfect structure of UiO-66 (i.e., 54.6 wt%); and *CN* is the coordination number of zirconium clusters. In the ideal structure of UiO-66-Zr, the coordination number is 12.

TablaS1. Results of N_2 adsorption analysis of UiO-66 and UiO-66-NH_2 catalysts with different number of defects

Catalyst	Area BET[a] (m^2g^{-1})	Pore volume[b] (cm^3g^{-1})
UiO-66 -12.4%	1262	0.47
UiO-66 -15%	1217	0.45
UiO-66 -25.6%	1027	0.38
UiO-66-NH_2 -14.8%	938	0.36
UiO-66-NH_2 -15.2%	935	0.36
UiO-66-NH_2-18%	1034	0.39

[a] For the calculation of the Brunauer-Emmett-Teller (BET) specific surface areas, the 0.005-0.06 P/P_0 pressure range of the isotherm was used to fit the data. Within this range, all the Rouquerol[2] consistency criteria are satisfied.
[b] Micropore volume obtained by the t-plot method.

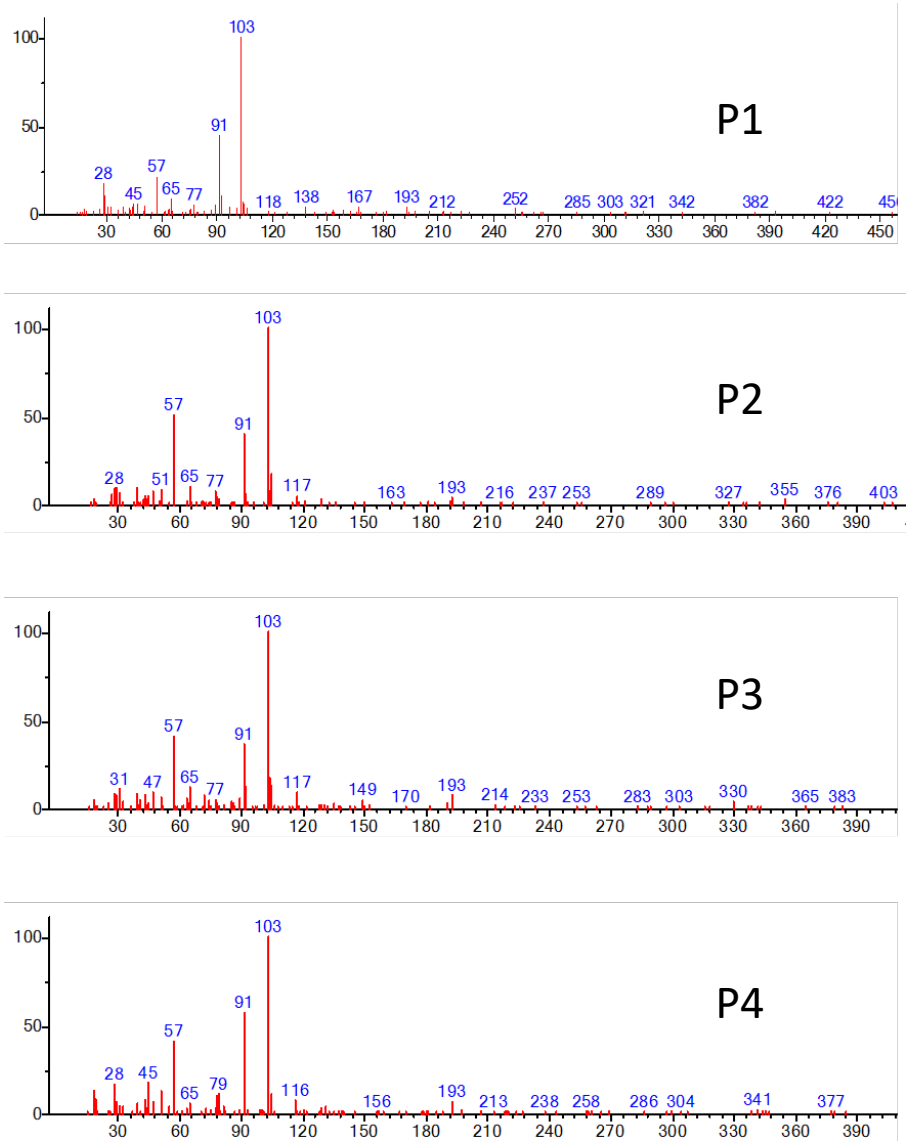

Figure S4. MS spectra of phenylacetaldehyde glycerol acetals. P1 and P4: *E* and *Z*-1,3-dioxanes; P2 and P3: *E* and *Z*-1,3-dioxolanes.

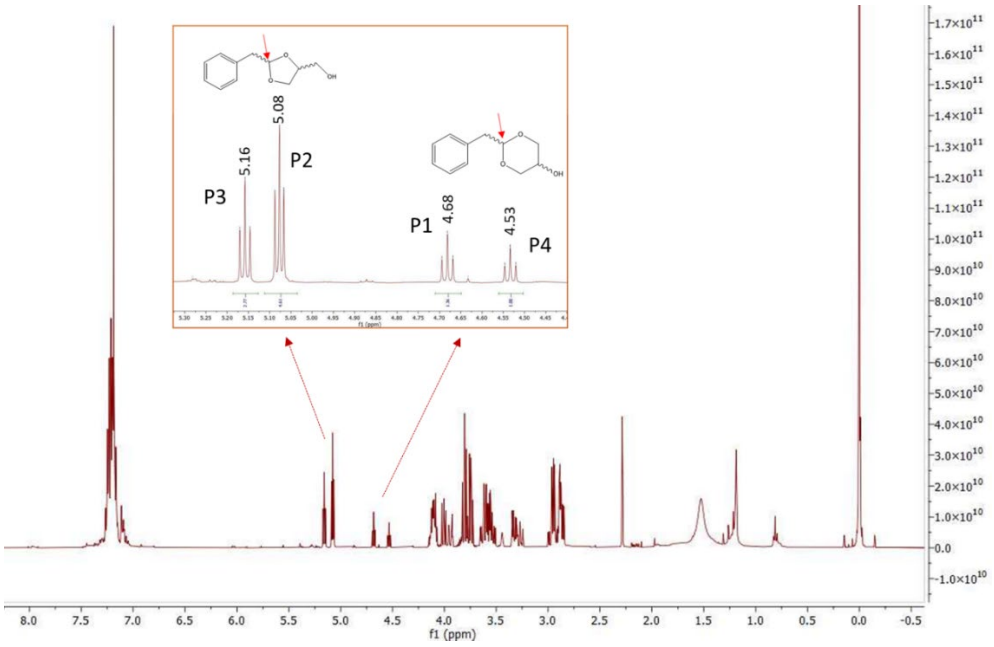

Figure S5. ^{1}H-RMN spectra of phenylacetaldehyde-glycerol acetalization products: P2 /P3 are *E/Z* 1,3-dioxolanes; P1/P4 are *E/Z* 1,3-dioxanes.

Table S2. Results of ^{1}H-RMN and GC quantitative analysis of phenylacetaldehyde-glycerol acetalization products

Product	Acetal	δ (ppm) (RMN)	Yield % (RMN)	Ret.time, min (GC)	Yield % (GC)
1,3-dioxane	P1	*t*, 4.68	13.9	13.02	13.8
	P4	*t,* 4.53	10.2	13.55	9.5
1,3-dioxolane	P2	*t*, 5.08	47.3	13.07	47.8
	P3	*t*, 5.16	28.6	13.27	28.9

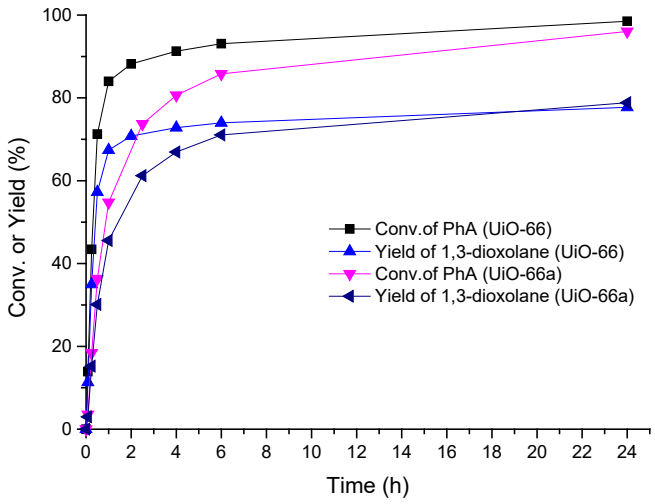

Figure S6. Conversion & time and Yield &time plots for acetalization reaction of phenylacetaldehyde with glycerol in presence of hydrated UiO-66 and UiO-66a dehydrated at 150°C under vacuum conditions (2h) before reaction. Reaction conditions: PhA (2 mmol), Gly (4 mmol), MOF (1.5 mol%Zr) 10 mg, reflux of toluene (6 mL), Dean Stark.

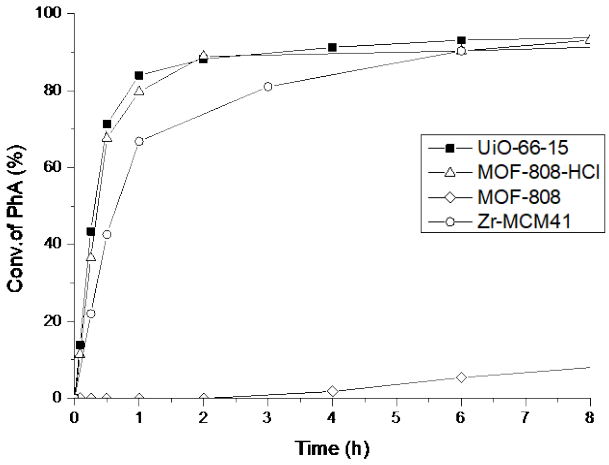

Figure S7. Conversion & time plots for acetalization reaction of phenylacetaldehyde with glycerol in the presence of various Zr-containing catalysts.

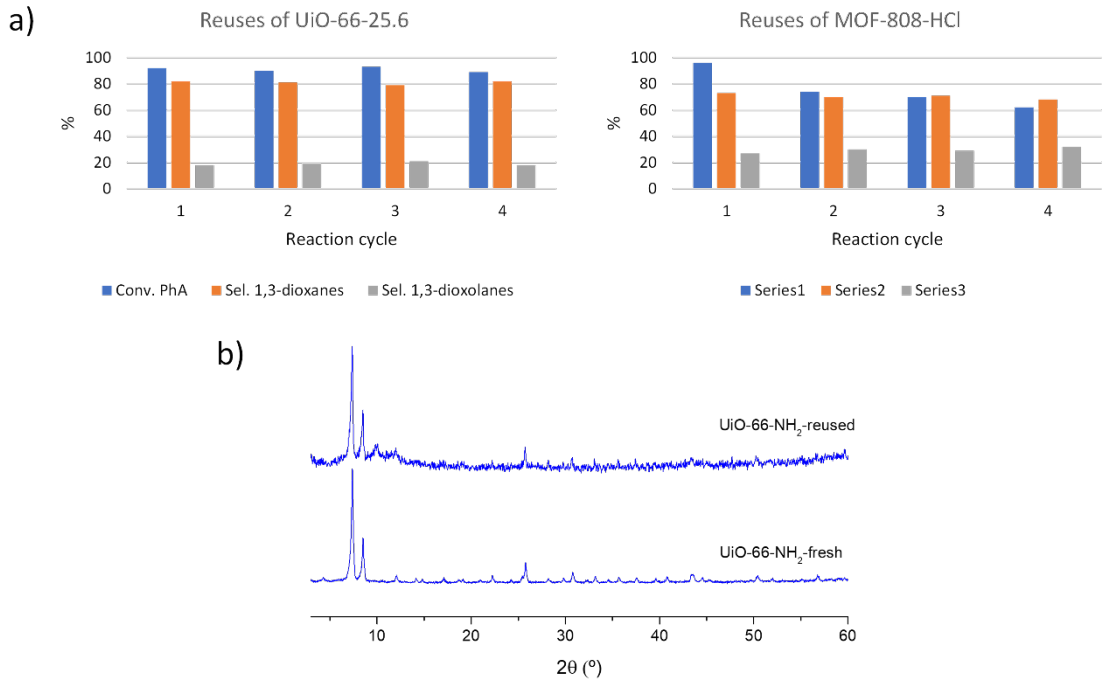

Figure S8. a) Results of consecutive reuses of UiO-66-25.6 and MOF-808-HCl samples in acetalization reaction of phenylacetaldehyde with glycerol after 6 h. b) XRD patterns of UiO-66-NH_2-18 catalyst before (fresh) and after being used in reaction for four consecutive cycles.

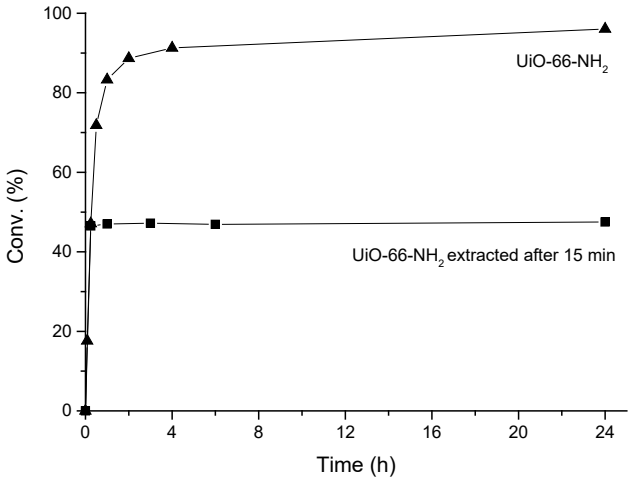

Figure S9. Conversion & time plots for acetalization reaction of phenylacetaldehyde with glycerol in presence of UiO-66-NH_2 (▲) and after removal of UiO-66-NH_2 (■) at 15 min of reaction.

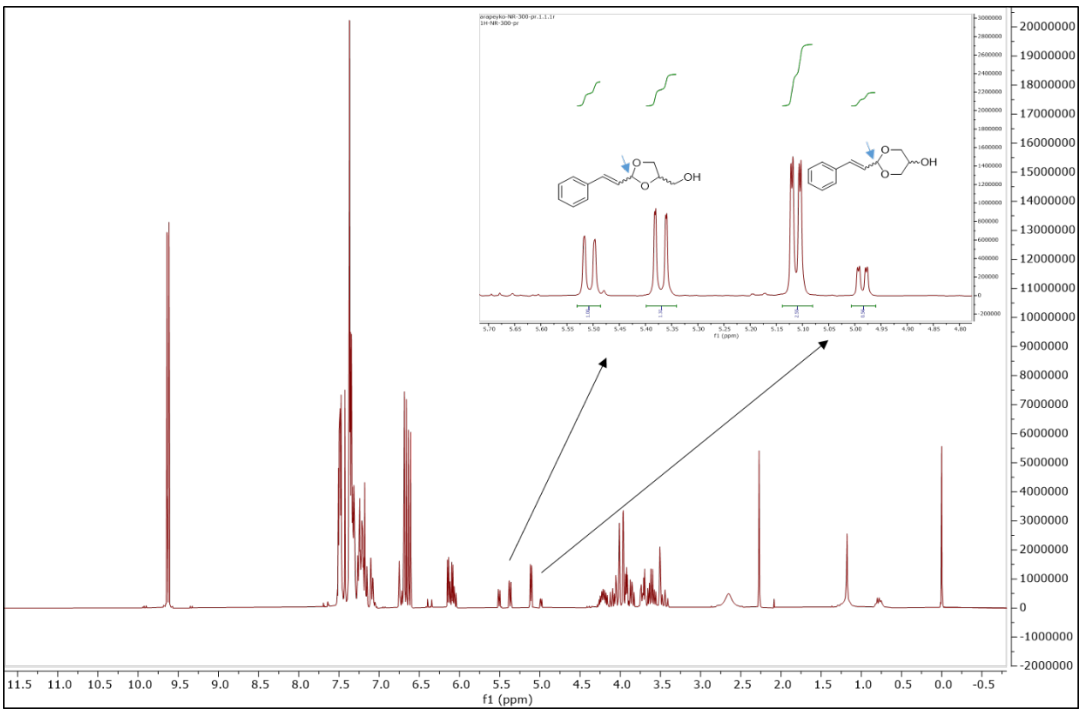

Figure S10. ^{1}H-NMR spectrum of cinnamaldehyde-glycerol acetalization products.

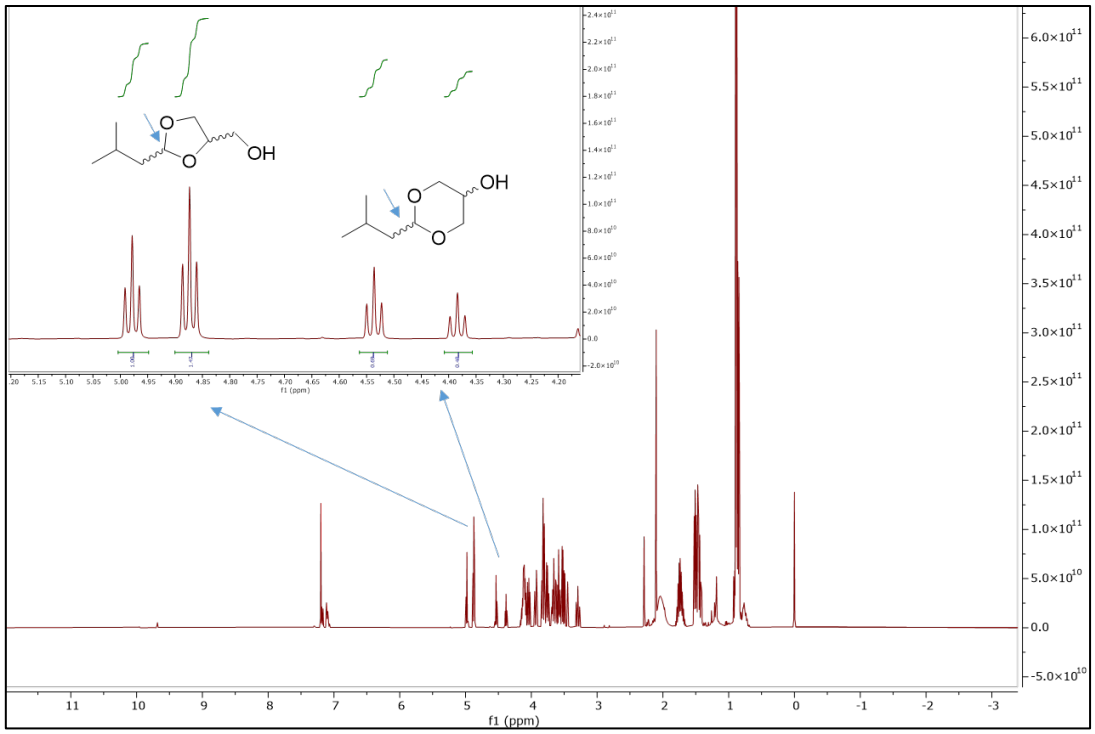

Figure S11. ^{1}H-NMR spectrum of isovaleraldehyde-glycerol acetalization products.

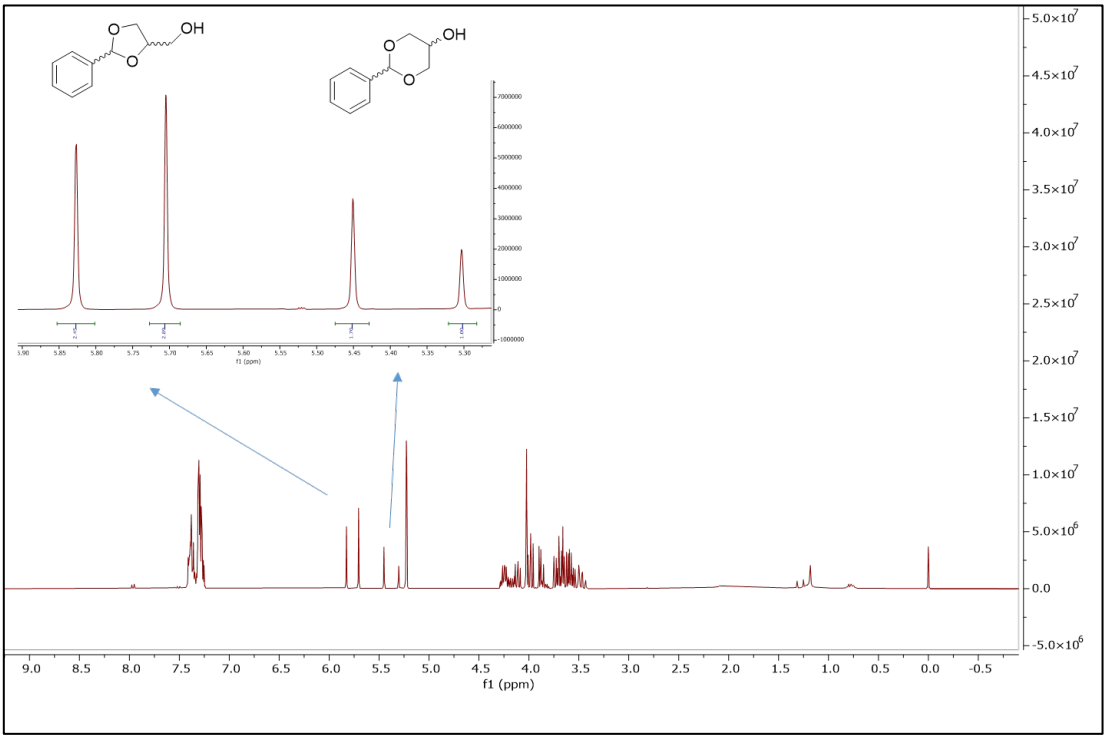

Figure S12. ^{1}H-NMR spectrum of benzaldehyde-glycerol acetalization products.

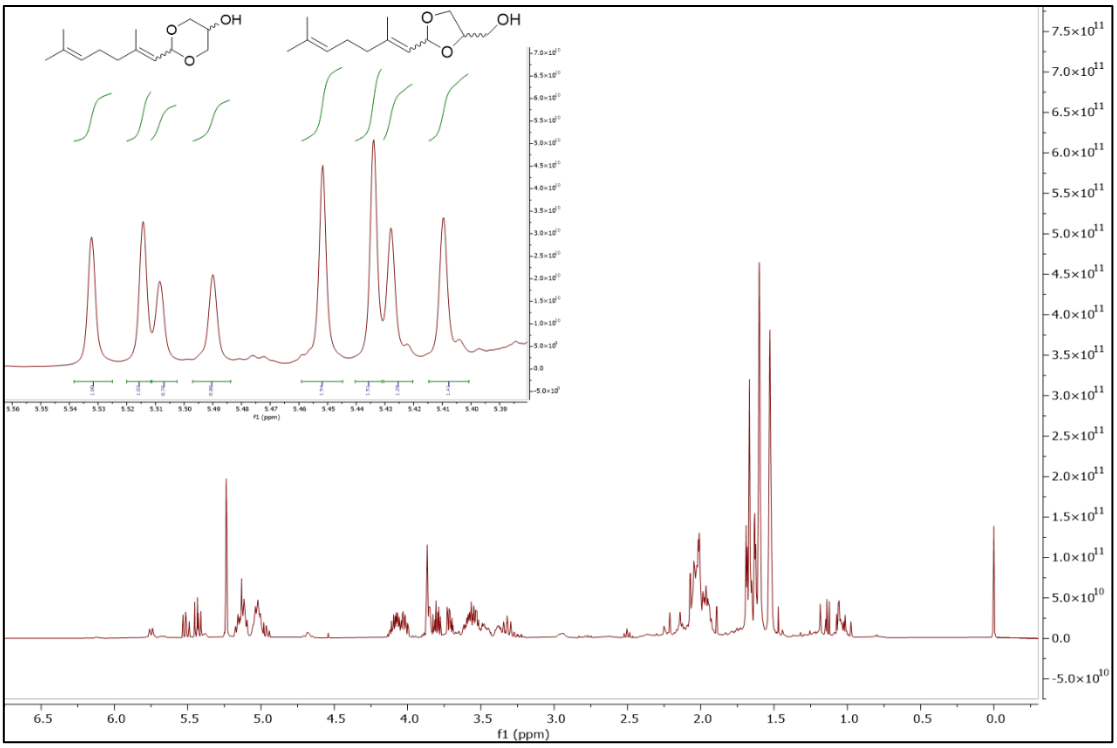

Figure S13. ^{1}H-NMR spectrum of citral (mixture of neral and geranial)-glycerol acetalization products.

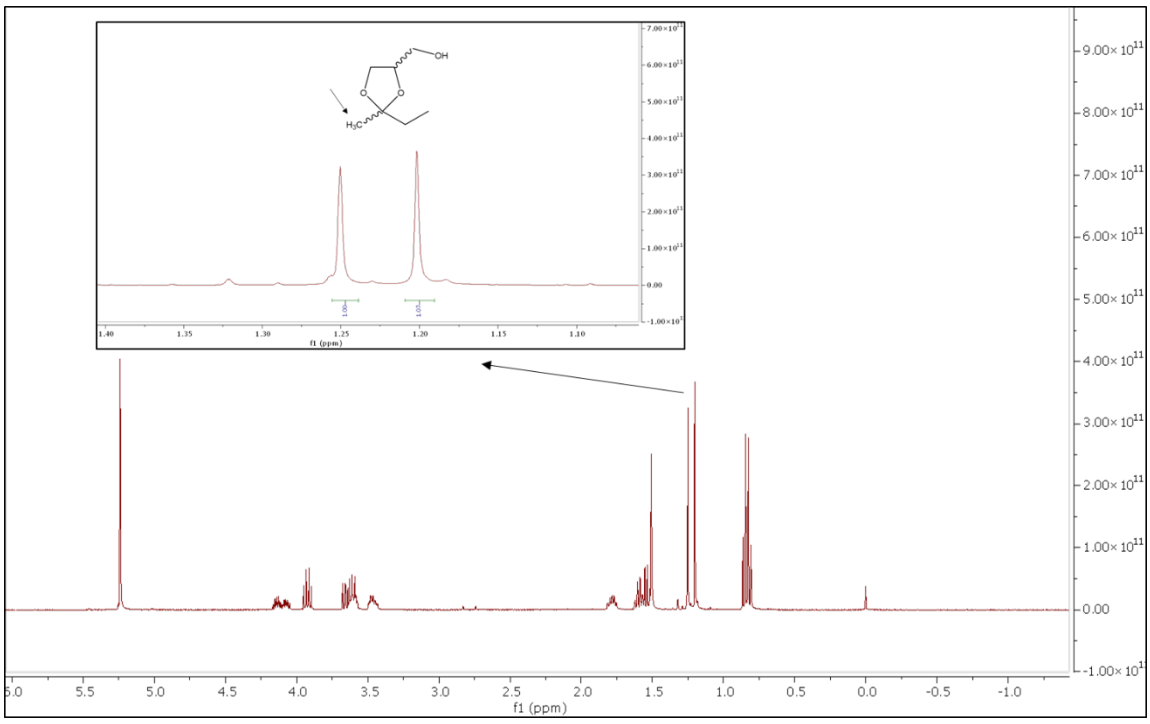

Figure S14. ^{1}H-NMR spectrum of 2-butanone -glycerol acetalization products.

References

1 L. Valenzano, B. Civalleri, S. Chavan, S. Bordiga, M. H. Nilsen, S. Jakobsen, K. P. Lillerud and C. Lamberti, *Chemistry of Materials*, 2011, **23**, 1700–1718.

2 J. Rouquerol, P. Llewellyn and F. Rouquerol, *Studies in Surface Science and Catalysis*, 2007, **160**, 49–56.